

Complete assignment of 3D spin axes of antiferromagnetic domain structures of NiO: Combined study of MLD-PEEM and cluster model calculation

Micromagnetic structures, i.e., magnetic domain structures, are strongly correlated with the magnetic nature of materials. The investigation of magnetic domain structures is very important not only for ferromagnetic (FM) materials but also for antiferromagnetic (AF) materials, from both applied and fundamental scientific points of view, for example, exchange bias. NiO is considered to be one of the typical AF materials. A detailed study of NiO will enable a complete understanding of AF domain structures. NiO has a relatively high Néel temperature ($T_N=523$ K) and a collinear spin structure. Owing to their magnetostriction caused by AF ordering, NiO samples below T_N consist of many twinned crystals. Crystallographic twinning leads to four different possible domains, the so-called twin domains (T-domains), with different contractions along the $\langle 111 \rangle$ axes. Each T-domain has three easy spin axes, i.e., the $\langle 112 \rangle$ directions. Thus, in a single T-domain, three different spin domains (S-domains) can exist. These 12 possible types of easy spin axis make the domain structures in NiO complicated. To understand the AF domain structures, both the T- and S-domains should be assigned. Although many studies have been carried out to observe the domain structures of NiO over the past five decades, no complete determination of the spin axes in each domain structure has been achieved. In the present study, we have successfully assigned the three-dimensional (3D) spin axes of these domain structures completely for the first time by a combined method of X-ray magnetic- and nonmagnetic linear dichroism (XMLD and XLD, respectively), photoemission electron microscopy (PEEM), and cluster model calculation including crystal symmetry [1].

The experiments were performed using two PEEM apparatuses installed at beamlines **BL17SU** and **BL25SU**. Here, we show the results obtained mainly at BL17SU, where *s*- and *p*-linearly polarized light is used. The PEEM apparatus at BL17SU is a spectroscopic photoemission and low-energy electron microscope (SPELEEM). A single-crystal NiO sample was cleaved at the (100) plane in atmosphere and then immediately transferred into a vacuum chamber.

Figure 1 shows the X-ray absorption spectra (XAS) obtained at the (a) O *K* and (b) Ni *L*₂ edges. It is confirmed that large XLD and XMLD arise at the photon energies indicated by arrows in Figs. 1(a) and 1(b), respectively. Thus, we obtained XLD- and XMLD-PEEM images at these photon energies by both *s*- and *p*-polarized lights. It was reported in Ref. [2]

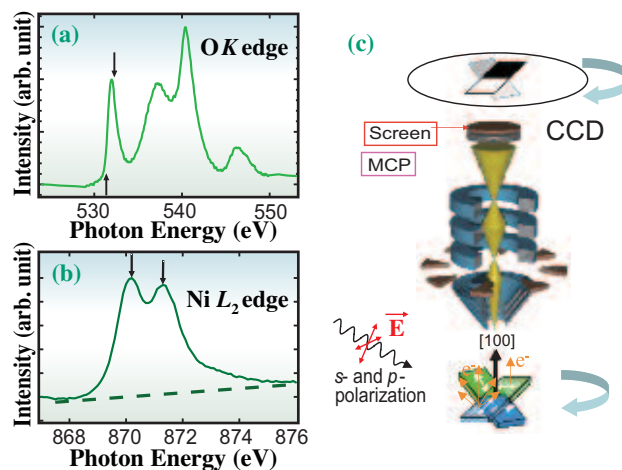


Fig. 1. (a) X-ray absorption spectrum (XAS) of NiO in O *K* edge region. PEEM images were acquired at photon energies indicated by arrows. (b) As (a) but in Ni *L*₂ edge region. The dashed line indicates the linear background considered in the observed absorption spectrum. (c) Schematic experimental setup for XLD- and XMLD-PEEM studies. The NiO(100) single crystal surface is azimuthally rotated around the [100] axis against the polarization vector. The AF domain contrast changes as a function of rotational angle.

that an XLD image reflects T-domain structures and an XMLD image reflects T- and S-domain structures. It is also known that the XMLD contrast depends on the angle between the polarization vector and the magnetization (spin axis). This means that we can determine the spin axis from the detailed angle dependence of XMLD-PEEM images. As shown in Fig. 1(c), we observed the azimuthal angle dependence (AAD) of the intensity ratio of the two peaks at the Ni *L*₂ edge in the S-domains with *s*- and *p*-polarized light sensitive to both parallel and perpendicular magnetization components, respectively, by rotating the sample around the [100] direction. We assigned the S-domains correctly by comparing the AAD with a cluster model calculation including the crystal symmetry.

The images shown in Fig. 2 are acquired with *p*-polarized light. At the O *K* edge, four types of contrast are observed corresponding to the four types of T-domain due to $\langle 111 \rangle$ crystal distortion, as shown in Fig. 2(a). The four colored lines in Fig. 2(b) indicate the boundaries of the four T-domains in the image. Here, we focus on the T-domain surrounded by the black line shown in Fig. 2(b). The three types of XMLD contrast at the Ni *L*₂ edge can be seen in the T-domain in Fig. 2(c). This suggests that the observed contrasts originate from the different S-domains. Therefore, the areas surrounded by three solid lines (green, blue, and red) in Fig. 2(d) correspond to the three types of S-

domain (S1, S2, and S3), i.e., three types of S-domain exist within a single T-domain. The observed XMLD in the three types of S-domain in the T-domain can easily be compared with the theoretical results in contrast to that in one type of S-domain in the T-domain, because the spin axes should exist within a specified (111) plane. As shown in Fig. 2(c), the boundaries of the S-domains are curved or unclear unlike the T-walls in Fig. 2(a).

Figures 3(a) and 3(b) show the Ni L_2 intensity ratio (higher/lower photon energy) dependence on azimuthal angle observed in the three types of S-domain in Fig. 2 with (a) s - and (b) p -polarized light. It has been considered for a long time that the XMLD contrast follows the $(3 \cos^2 \theta - 1)$ dependence, where θ is the angle between a polarization vector and a spin. However, this was refuted very recently [3]. The AAD should be explained by considering the crystal symmetry. Therefore, we performed an analysis using a NiO_6 octahedral cluster model, where the crystal symmetry and the full multiplet splitting of the Ni ion are considered [4]. Figures 3(c) and 3(d) show the results obtained by NiO_6 cluster calculation for s - and p -polarized light excitations, respectively. The details of the model and the parameters for NiO are described in Refs. [1] and [4]. In Figs. 3(c) and 3(d), the intensity ratios of the three types of easy axis ($[\bar{1}21]$ (green), $[2\bar{1}1]$ (blue), $[112]$ (red)) in the $[11\bar{1}]$ T-domain are calculated. As shown in Fig. 3, the AADs of the relative intensity ratios are in qualitative agreement between the experiments and the calculations. From

these comparisons, the easy axes for S1, S2, and S3 can be determined as above. Thus, the observed AAD of XMLD in the three S-domains can be explained by the cluster calculation.

An analytic formula that relates the intensity ratio to the spin axis was also derived. This formula is essential for understanding the behavior of XMLD in NiO. We further observed all types of the T- and S-walls. The results gave us an important basis for understanding antiferromagnetism and ferromagnetic/AF exchange coupled systems.

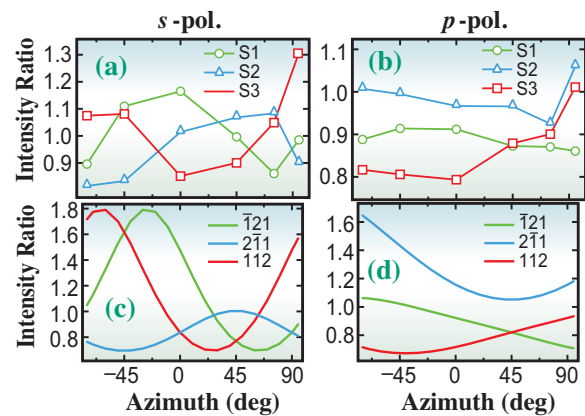


Fig. 3. (a) AAD (see text) of absorption intensity ratios at Ni L_2 edge in three domains [shown in Fig. 2(d)] observed with s -polarized light. The projective components of the propagation vector of the incident light to the surface plane are the $[001]$ direction at 0° and $[010]$ direction at 90° . (b) As (a) but with p -polarized light. (c) Calculated absorption intensity ratios (higher/lower energy) of Ni L_2 edge with s -polarized light by the cluster calculation containing full multiplet splitting including crystal symmetry. The results of the three spin easy axes, namely, $[\bar{1}21]$, $[2\bar{1}1]$, and $[112]$, are presented. (d) As (c) but with p -polarized light.

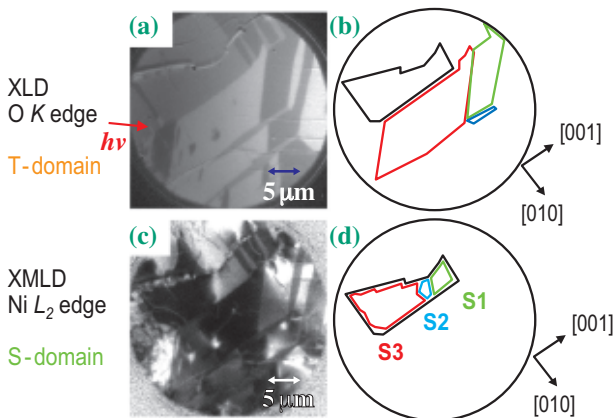


Fig. 2. PEEM images obtained by dividing two images acquired at two photon energies (higher $h\nu$ image/lower $h\nu$ image) with the p -polarized light shown in Fig. 1. (a) T-domain structures observed by XLD-PEEM. The red arrow indicates the incident soft X-ray direction projected onto the surface plane. (b) Schematic domain structures of (a). The four colored solid lines indicate the boundaries of the four T-domains. The area surrounded by a black solid line corresponds to the single T-domain discussed here. (c) S-domain structures observed by XMLD-PEEM observed at the same locations as (a). (d) Schematic domain structures of (c). The areas surrounded by solid lines (S1, S2, and S3) correspond to the three S-domains in the single T-domain indicated by the black line shown in (b).

Kuniaki Arai^a, Arata Tanaka^b and Toyohiko Kinoshita^{c,d,*}

^aSRL-ISSP, The University of Tokyo

^bADSM, Hiroshima University

^cSPring-8/JASRI

^dCREST, JST

*E-mail: toyohiko@spring8.or.jp

References

- [1] K. Arai, T. Okuda, A. Tanaka, M. Kotsugi, K. Fukumoto, T. Ohkouchi, T. Nakamura, T. Matsushita, T. Muro, M. Oura, Y. Senba, H. Ohashi, A. Kakizaki and T. Kinoshita: *J. Phys. Soc. Jpn.* **79** (2010) 013703 and *Erratum J. Phys. Soc. Jpn.* **79** (2010) 038001.
- [2] T. Kinoshita *et al.*: *J. Phys. Soc. Jpn.* **73** (2004) 2932.
- [3] For example, E. Arenholz *et al.*: *Phys. Rev. Lett.* **98** (2007) 197201.
- [4] A. Tanaka and T. Jo: *J. Phys. Soc. Jpn.* **63** (1994) 2788.